Calcium-Dependent Binding of Annexin 12 to Phospholipid Bilayers: Stoichiometry and Implications†

D. R. Patel,‡ C. C. Jao,‡ W. S. Mailliard,‡ J. M. Isas,‡ R. Langen,§ and H. T. Haigler*,‡

Department of Physiology and Biophysics, University of California, Irvine, California 92697, and Department of Biochemistry and Molecular Biology, University of Southern California, Los Angeles, California 90033

Received February 19, 2001; Revised Manuscript Received April 25, 2001

ABSTRACT: Annexins (ANXs) are a superfamily of proteins whose functional hallmark is Ca^{2+}-dependent binding to anionic phospholipids. Their core domains are usually composed of a 4-fold repeat of a conserved amino acid sequence, with each repeat containing a type II Ca^{2+} binding site that is generally thought to mediate Ca^{2+}-dependent binding to the membrane. We now report that ANX12 binding to phospholipid vesicles is highly cooperative with respect to Ca^{2+} concentration (Hill constant $\sim$ 7), thereby suggesting that more than the four well-characterized type II Ca^{2+} binding sites are involved in phospholipid binding. Two independent approaches, a novel $^{45}Ca^{2+}$ copelleting assay and isothermal titration calorimetry, indicate a stoichiometry of $\sim$12 mol of Ca^{2+}/mol of ANX12 for binding to phospholipid vesicles. On the basis of the "low-affinity" Ca^{2+}-binding sites in a number of ANX X-ray crystal structures, we propose a model for ANX12 bilayer binding that involves three types of Ca^{2+} sites in each of the four repeats. In this model, there is a complementarity between the spacing of the ANX12 Ca^{2+} binding sites and the spacing of the phospholipid headgroups in bilayers. We tested the implications of the model by manipulating the physical state of vesicles composed of phospholipids with saturated acyl chains with temperature and measuring its influence on ANX12 binding. ANX12 bound to vesicles in a Ca^{2+}-dependent manner when the vesicles were in the liquid crystal phase but not when the phospholipid was in the gel phase. Furthermore, ANX12 bound initially to fluid bilayers remained bound when cooled to 4 °C, a temperature that should induce the gel phase transition. Overall, these studies suggest that ANX12 is well suited to being a Ca^{2+} sensor for rapid all-or-none intercellular membrane-related events.

The annexins (ANXs)[1] comprise a superfamily of proteins that undergo high-affinity Ca^{2+}-dependent binding to anionic phospholipids that are preferentially localized to the cytosolic face of plasma membranes (*1*). They have been implicated in a number of membrane-related intracellular events, including membrane fusion and vesicular trafficking (*2*). Each ANX contains a structurally conserved core domain that consists of a 4-fold (8-fold in the case of ANX6) repeat of a homologous 70-amino acid sequence that contains the Ca^{2+} binding sites (*1*). Each ANX also contains a nonconserved N-terminal domain that often has sites for post-translational modification (*1*).

High-resolution X-ray crystal structures are available for the soluble form of several different ANXs, and all core domains have essentially the same backbone fold (*3*). Each of the four repeats in the core domain contains five α-helices, named A−E, and the domains pack together to form a slightly curved disklike structure. Helices A and B and helices D and E form helix−loop−helix folds in each of the four repeats, and the eight loops formed by these motifs are on the convex face of the disk. These loops mediate Ca^{2+}-dependent binding to the periphery of membranes by a bridging mechanism in which coordination sites for Ca^{2+} are provided by the protein and by phospholipid polar headgroups (*1*). X-ray crystallography studies of the soluble form of ANXs (*4*−*10*) and functional analysis of site-directed mutants (*2*) indicate that the primary Ca^{2+} binding site is the "type II" site in which Ca^{2+} coordination is jointly mediated by the loop between helices A and B and by the loop between helices D and E. In addition, certain ANX crystal structures contain "low-affinity" or "secondary" Ca^{2+} sites whose function in membrane binding has not been extensively characterized (*1*). The reported values of Ca^{2+} stoichiometry for membrane-bound ANXs vary wildly, but some data support the idea that the secondary Ca^{2+} sites participate in membrane binding (*11*). However, little is known about the structure of ANXs on membranes, and current models of Ca^{2+}-dependent interaction of ANXs with membranes often consider only the involvement of the type II sites (*12*).

The following studies provide a tantalizing view of ANX structure on membranes. Electron crystallography studies of two-dimensional crystals of membrane-bound ANX5 revealed an extended lattice of trimers (*13*, *14*). A similar

† This work was supported by National Institutes of Health Grants GM-55651 (to H.T.H.), GM57998 (in partial support of D.R.P.), and GM07311 (predoctoral training grant to D.R.P.).

* To whom correspondence should be addressed: Department of Physiology and Biophysics, University of California, Irvine, CA 92697. Phone: (949) 824-6304. Fax: (949) 824-8540. E-mail: hhaigler@uci.edu.

‡ University of California.

§ University of Southern California.

[1] Abbreviations: ANX, annexin; PS, phosphatidylserine; PG, phosphatidylglycerol; PC, phosphatidylcholine; DMPS, dimyristoylphosphatidylserine; DMPG, dimyristoylphosphatidylglycerol; DTPC, ditridecanoylphosphatidylcholine; ITC, isothermal titration calorimetry.

10.1021/bi010345+ CCC: $20.00
Published on Web 05/25/2001

arrangement was visualized on supported lipid bilayers using atomic force microscopy (*15*). Comparison of the X-ray crystal structure of soluble ANX5 with the electron microscopy structure of the membrane-bound protein indicated that a hingelike motion between repeats 1 and 4 and repeats 2 and 3 allowed the type II sites on the convex face of the protein to become coplanar in the membrane-bound form (*5*). Although these methods reveal some of the general features of membrane-bound ANX5, the low-resolution images do not provide structural details.

We recently used hydra ANX12 (*16*) as a model for studying ANX structure and function with particular emphasis on using a site-directed spin labeling approach to obtain atomic-resolution structural information about the membrane-bound protein. The sequence of the core domain of ANX12 is ~50% identical with that of any given mammalian ANX (*16*), and its X-ray crystal structure reveals a nearly identical backbone fold (*7*). ANX12 shares many properties with ANX5, including the formation of Ca^{2+}-dependent trimers on the surface of phospholipid bilayers (*17*, *18*). In fact, hydra ANX12 and human ANX5 efficiently form heterotrimers (*18*). Both ANX12 and -5 appear to be able to refold and insert into membranes in a Ca^{2+}-independent manner at low pH (*19*−*21*), but the experiments reported herein focus on the Ca^{2+}-dependent peripheral membrane form of ANX12.

It is becoming increasingly clear that Ca^{2+}-dependent interaction between ANXs and membranes alters the structure of both the membrane (*22*) and the protein (*18*) and that these changes may be at the core of the biological function of ANXs. The purpose of this study is to define key biochemical and biophysical characteristics of the Ca^{2+}-dependent binding of ANX12 to phospholipid bilayers. We obtained data that are not consistent with current models that envision four Ca^{2+}-binding sites mediating ANX binding to phospholipid bilayers. On the basis of our data, we propose a model in which the interaction of ANX12 with the surface of bilayers is more extensive than was generally assumed. This model explains many of the observed effects of ANXs on bilayers and provides a framework for asking key questions concerning the biological function of this superfamily of proteins.

MATERIALS AND METHODS

Materials. Recombinant ANX12 was expressed in bacteria and purified by reversible Ca^{2+}-dependent binding to phospholipid vesicles followed by column chromatography according to previously published protocols (*16*). The ANX12 concentration was determined from the absorbance (ϵ_{280} = 12 288 M^{-1} cm^{-1}). The following preparations of lipids were obtained from Avanti Polar Lipids (Alabaster, AL) and were used to make large unilammelar vesicles by the method of Reeves and Dowben (*23*): phosphatidylserine (PS, brain, catalog no. 840037), phosphatidylglycerol (PG, 16:1, 18:1, catalog no. 840457), and phosphatidylcholine (PC, egg yolk, catalog no. 850355). In certain experiments, vesicles were prepared from phospholipids with saturated acyl chains: dimyristoylphosphatidylserine (DMPS, 14:0, catalog no. 840033), dimyristoylphosphatidylglycerol (DMPG, 14:0, catalog no. 840435), and ditridecanoylphosphatidylcholine (DTPC, 13:0, catalog no. 850340). The ratios of phospholipids are reported on a weight to weight basis. The Ca^{2+} source for stoichiometry experiments was the $CaCl_2$ standard from Thermo Orion (Beverly, MA).

Table 1: Ca^{2+}-Dependent Binding of ANX12 to Vesicles with Various Lipid Compositions[a]

vesicle composition	[Ca^{2+}] (mM)	stoichiometry	SD (*n*)
2:1 PS/PC	150	10.7	0.4 (8)
2:1 PG/PC	150	12.9	1.4 (4)
1:2 PA/PC	250	12.1	0.3 (4)
2:1 DMPS/DTPC	150	11.9	1.6 (2)
2:1 DMPG/DTPC	150	13.4	1.3 (4)

[a] ANX12 (50 μg) was incubated for 15 min with the indicated concentration of $^{45}Ca^2$ and phospholipid vesicles of the indicated composition (1:5 protein:phospholipid ratio by weight). Samples containing saturated lipids [PS, bovine brain phosphatidylserine; PG, phosphatidylglycerol (16:1, 18:0); PC, egg yolk phosphatidylcholine] were incubated at 25 °C, while samples containing unsaturated lipids [DMPS, dimyristoylphosphatidylserine (14:0); DMPG, dimyristoylphosphatidylglycerol (14:0); DTPC, ditridecanoylphosphatidylcholine (13:0)] were incubated at 37 °C. The Ca^{2+} binding stoichiometry (moles of Ca^{2+} per mole of ANX12) was determined in the copelleting assay as described in Materials and Methods.

Copelleting Assay. Unless otherwise indicated, the standard copelleting assay contained phospholipid vesicles equilibrated in Hepes buffer (20 mM, pH 7.4, containing 100 mM NaCl) with the indicated concentration of $CaCl_2$. After a 15 min incubation with the indicated amount of ANX12 at 25 °C, the vesicles were pelleted by centrifugation (16000*g* for 5 min). Pellets including bound protein are separated from the supernatant containing unbound protein for further analysis.

In certain experiments, aliquots of the supernatants were transferred to Immobilon PVDF membranes using a slot blot apparatus and then stained with Coomassie blue. The samples, along with a standard curve of known concentrations of ANX12, were analyzed by densitometry.

A modification of the standard copelleting assay was used with $^{45}Ca^{2+}$ to quantify the stoichiometry for Ca^{2+}-dependent binding of ANX12 to vesicles. This assay contained ANX12 (50 μg) and vesicles (1:5 ratio of protein to phospholipid by weight) in a 1 mL final volume of 100 mM Tris-HCl (pH 7.5) with the indicated $^{45}Ca^{2+}$ concentration. The specific activity of the $^{45}Ca^{2+}$ in each sample was 1.1−1.4 nCi/nmol. Following centrifugation, the pellets and supernatants were subjected to liquid scintillation counting to determine the total amount of $^{45}Ca^{2+}$ bound to the vesicles. The level of nonspecific binding of $^{45}Ca^{2+}$ to the vesicles was determined in parallel samples in the absence of ANX12 and subtracted from the total counts to give the level of ANX12-dependent binding. Under the various conditions described in Table 1, the level of nonspecific binding was between 12 and 25% of the total level of binding. The pellets of parallel samples were analyzed to determine the amount of ANX12 in the pellet. The Ca^{2+}-binding data are expressed as the moles of Ca^{2+} per mole of ANX12 in the pellet. In most experiments, the concentration of Ca^{2+} used in the assay induced binding of approximately 95% of the added ANX12.

Isothermal Titration Calorimetry. Isothermal titration calorimetry (ITC) experiments were performed on an ultrasensitive Microcal MCS-ITC instrument (Microcal, Inc., Northampton, MA). All components in the system were exchanged into thoroughly degassed HEPES buffer (100 mM, pH 7.5). The 1.37 mL sample cell, equilibrated to 25 °C, contained 25 μM ANX12 and 10 μg of PS/PC (2:1)

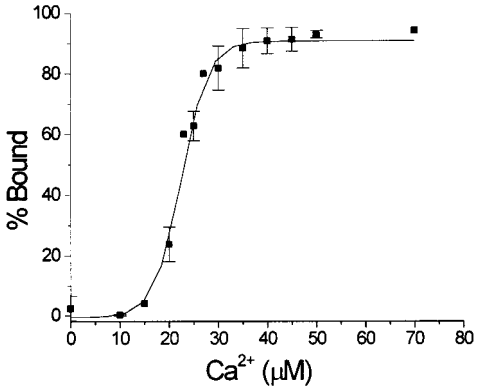

FIGURE 1: ANX12 Ca^{2+}-dependent vesicle binding curve. Annexin 12 (4 μg) was bound to phospholipid vesicles (2:1 PS/PC, 200 mg) at the indicated Ca^{2+} concentration. ANX12 bound to vesicles was separated from the unbound protein by centrifugation to pellet the vesicles. The amount of bound protein (expressed as a % of total added) was determined by densitometric analysis of triplicate samples on Coomassie blue-stained blots (see Materials and Methods). When the data for binding between 15 and 30 μM Ca^{2+} were replotted by the method of Hill (*34*), a slope of 7.0 and an intercept of 23 μM Ca^{2+} were obtained.

phospholipid vesicles. The sealed reference cell contained water. Control experiments consisted of either buffer only, vesicles and buffer, or annexin and buffer. A motorized titration syringe was used to add 5 μL aliquots of $CaCl_2$ (5 mM) to the sample cell. Thirty-two injections were made at 400 s intervals while stirring at 400 rpm. The rate of heat released after each injection of Ca^{2+} into the sample was measured and subsequently analyzed on Origin 5.0 software. The ITC experiments whose results are reported in Figure 2 in HEPES buffer were repeated ($n = 3$) in Tris-HCl buffer (100 mM, pH 7.5). When Tris buffer was used, a moderate amount of heat was released when phospholipid vesicles were titrated with Ca^{2+} in the absence of ANX12. However, when the titration curve for vesicles was subtracted from the one in the presence of vesicles and ANX12, the amount of ANX12-specific heat released was within experimental error of that reported in HEPES buffer.

RESULTS

Determination of Ca^{2+}-Dependent Vesicle Binding Affinity. The standard copelleting assay was used to evaluate Ca^{2+}-dependent binding of ANX12 to large unilamellar vesicles composed of PS and PC (2:1), a phospholipid mixture commonly used in annexin studies. No binding to phospholipid vesicles was observed in the absence of Ca^{2+}, and ~95% was bound when the Ca^{2+} concentration was >40 μM (Figure 1). Half-maximal vesicle association of ANX12 occurred at 23 μM Ca^{2+}. ANX12 binding to phospholipid vesicles was remarkably cooperative with a Hill coefficient of ~7.0, implying that more than the four well-characterized type II Ca^{2+} binding sites are involved in phospholipid binding.

Stoichiometry Measurements with Isothermal Titration Calorimetry. The interaction of ANX12 with Ca^{2+} and PS/PC (2:1) vesicles was studied by ITC. Control experiments in which up to 523 μM Ca^{2+} was titrated into a sample cell with only ANX12 resulted in an undetectable amount of released heat (not shown). Thus, like other annexins, ANX12 appears to have a very low affinity for Ca^{2+} in the absence of phospholipids. Figure 2A shows the results of a typical experiment in which PS/PC vesicles were titrated with Ca^{2+} in the presence (bottom trace) or absence (top trace, offset) of ANX12. Each downward spike shows the amount of heat

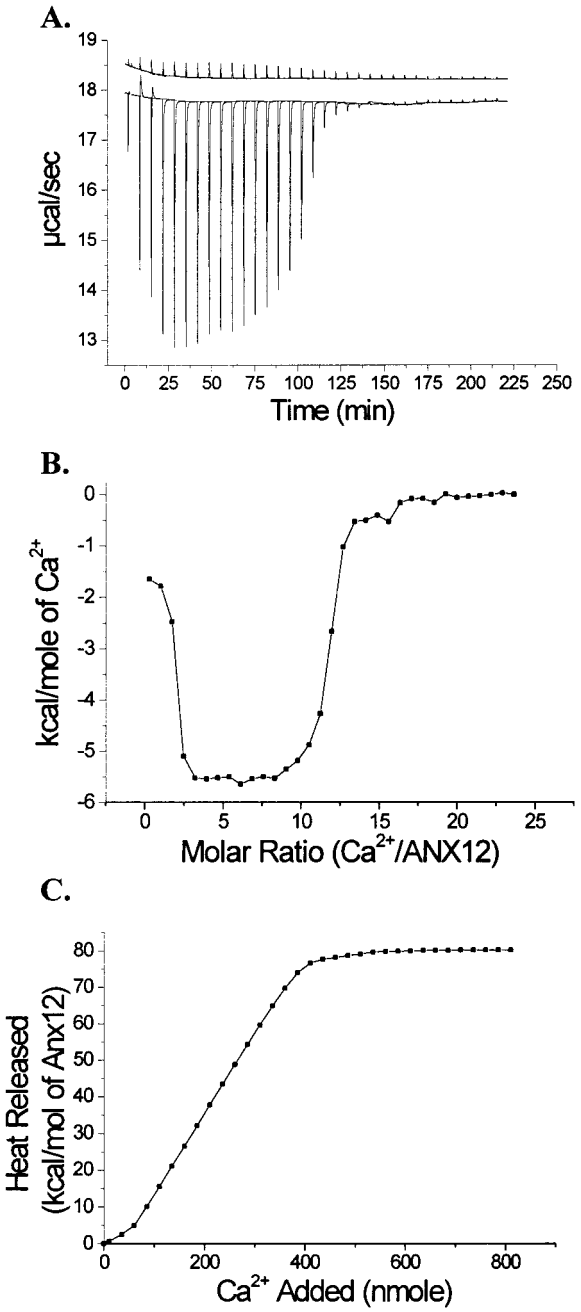

FIGURE 2: Isothermal calorimetric titration of ANX12 with Ca^{2+}. (A) Vesicles composed of PS and PC (2:1) were titrated with $CaCl_2$ in the presence (bottom trace) or absence (top trace, offset) of ANX12, as described in Materials and Methods. Each titration event consisted of a 5 μL addition. A 5 mM $CaCl_2$ solution was used and resulted in a downward spike, which indicates the release of heat. Control experiments in which $CaCl_2$ was titrated into a sample cell with only ANX12 or in which Ca^{2+}-free buffer was titrated into a sample cell with ANX12 and vesicles resulted in an undetectable amount of released heat (not shown). (B) The raw data in panel A were integrated, and the curve in the absence of ANX12 was subtracted from the one in the presence of the protein. The resulting ANX12-specific heat release curve is shown. The Ca^{2+} stoichiometry was analyzed as described in Materials and Methods. (C) The cumulative amount of ANX12-specific heat released as a function of the amount of added Ca^{2+}.

released over time after each titration event. An integration of the raw data provides the amount of heat released for the reaction. Figure 2B shows the amount of ANX12-specific heat released as a function of the amount of Ca^{2+} added and was obtained by subtracting the control from the experimental data shown in Figure 2A. The amount of ANX12-specific heat released can be divided into three stages. In the initial stage of the curve in Figure 2B, we interpret the increasing amounts of heat released during the first three injections as reflective of partial binding of ANX to the vesicles, which is a result of the free Ca^{2+} concentration being below the concentration required for maximal binding. The second stage is a plateau in which every aliquot of Ca^{2+} added results in a relatively constant, large amount of heat being released, suggesting that nearly all of the added Ca^{2+} is bound to ANX12 and the vesicles to form the ternary complex. Saturation of Ca^{2+}-binding sites is seen in the final stage of the reaction where additional injections of Ca^{2+} result in decreasing amounts of heat being released. This interpretation of the data was validated by analysis of parallel copelleting experiments using $^{45}Ca^{2+}$ (data not shown). Thus, the stoichiometry of binding could be calculated from the ITC data in Figure 2B by subtracting the amount of added Ca^{2+} required to produce the half-maximal response in the initial stage from the amount required to produce the ensuing half-maximal response in the final stage. Analysis of the data in Figure 2B and another identical experiment ($n = 2$) indicated a stoichiometry of 11 ± 0.5 mol of Ca^{2+} bound per mole of ANX12 monomer. The cumulative amount of heat released for the formation of the ternary complex (ANX12−Ca^{2+}−lipid) was -75 ± 5 kcal/mol of ANX12 (Figure 2C), indicating a highly exothermic reaction. Since the K_a for ANX association with bilayers in the presence of Ca^{2+} is known to be on the order of 0.1 nM (*24*), it is clear that the large exothermic enthalpy must be offset with a large decrease in entropy with major contributions likely coming from both the protein and phospholipid.

Stoichiometry Measurements with the $^{45}Ca^{2+}$ Copelleting Assay. The stoichiometry of Ca^{2+}-dependent binding of ANX12 to phospholipid vesicles was independently measured by a novel assay. ANX12 and vesicles were incubated in the presence of $^{45}Ca^{2+}$ at a cation concentration that induced maximal binding. The mixture was centrifuged to produce a small pellet of vesicles along with associated ANX12. The pellet was analyzed by liquid scintillation counting to determine the amount of bound $^{45}Ca^{2+}$. Using this assay, a stoichiometry of 10.7 ± 0.4 ($n = 8$) mol of Ca^{2+}/mol of ANX12 was determined with PS/PC (2:1) vesicles (Table 1). Similar values for the Ca^{2+} binding stoichiometry were obtained when the concentration of Ca^{2+} was lowered to a value at which the level of ANX12 binding began to decrease (data not shown).

Previous studies of several annexin gene products have shown that these proteins undergo Ca^{2+}-dependent binding to phospholipids containing a number of different anionic polar headgroups (*25*). Our preliminary studies demonstrated that ANX12 bound to vesicles containing PC and either PG or PA in a Ca^{2+}-dependent manner, similar to the binding observed to PS-containing vesicles (data not shown). Using the $^{45}Ca^{2+}$ copelleting assay, we determined that the Ca^{2+} binding stoichiometry was 12.9 ± 1.4 ($n = 4$) and 12.1 ± 0.3 ($n = 4$) mol of Ca^{2+}/mol of ANX12 for binding to PG- and PA-containing vesicles, respectively (Table 1). Thus, similar Ca^{2+} binding properties were observed with phospholipids composed of different anionic polar headgroups.

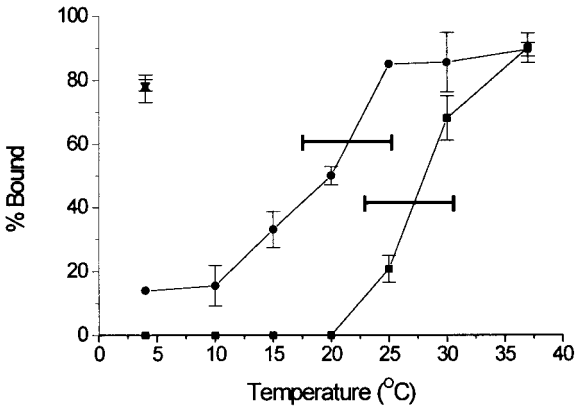

FIGURE 3: ANX12 binding to lipids at the phase transition temperature. Vesicles composed of equal amounts of DTPC and either DMPS (■) or DMPG (●) were incubated with 10 μg of ANX12. All samples are at 1:10 protein:lipid ratio by weight and were incubated and centrifuged at the indicated temperature according to the standard copelleting assay (see Materials and Methods) using Tris-HCl buffer (100 mM, pH 7.5) and either 50 or 100 μM Ca^{2+} for vesicles containing glycerol or serine headgroups, respectively. Duplicate samples were analyzed, and the percentage of added ANX12 that was associated with the pellet is shown along with the standard deviation. Black bars indicate the phospholipid phase transition temperature range as determined experimentally by differential scanning calorimetry in Tris-HCl buffer.. Control experiments carried out under the same conditions at 4 °C show ANX12 binding to vesicles composed of equal parts PC and either PS (▼) or PG (▲) which contain unsaturated acyl chains and remain in the liquid crystal phase at 4 °C.

Effects of Phospholipid Bilayer Fluidity on ANX12 Binding. The following experiments were designed to determine whether the physical state of bilayers influences ANX12 binding. Vesicles were prepared from phospholipids containing saturated acyl chains so the fluidity of the bilayer could be modulated by temperature. Preliminary experiments showed that vesicles composed of equal parts dimyristoyl-PS (DMPS, 14:0) and ditridecanoyl-PC (DTPC, 13:0) bound ANX12 in a Ca^{2+}-dependent manner at 37 °C similar to that of the well-characterized vesicles composed of PS and PC from biological sources which contain unsaturated acyl chains (data not shown). In the presence of Ca^{2+}, ANX12 bound to DMPS/DTPC vesicles equilibrated at 37 °C nearly quantitatively (Figure 3), with a Ca^{2+} stoichiometry (Table 1) similar to that obtained from vesicles made with unsaturated acyl chain phospholipids. Likewise, at 37 °C, vesicles containing PG with saturated acyl chains (DMPG/DTPC) bound ANX12 in a Ca^{2+}-dependent manner (Figure 3) and had a Ca^{2+} stoichiometry (Table 1) similar to those of vesicles containing PG with unsaturated acyl chains. In striking contrast, at 4 °C the level of ANX12 binding to DMPG/DTPC vesicles was <15% of the total protein and ~0% for DMPS/DTPC vesicles, while lowering the temperature had little effect on vesicles containing unsaturated phospholipids (Figure 3). Even high concentrations of Ca^{2+} (500 μM) did not significantly increase the level of binding of ANX12 to DMPS/DTPC or DMPG/DTPC vesicles at 4 °C (data not shown). As the temperature was increased from 4 to 37 °C, both DMPS/DTPC and DMPG/DTPC vesicles efficiently bound ANX12 at approximately the temperature

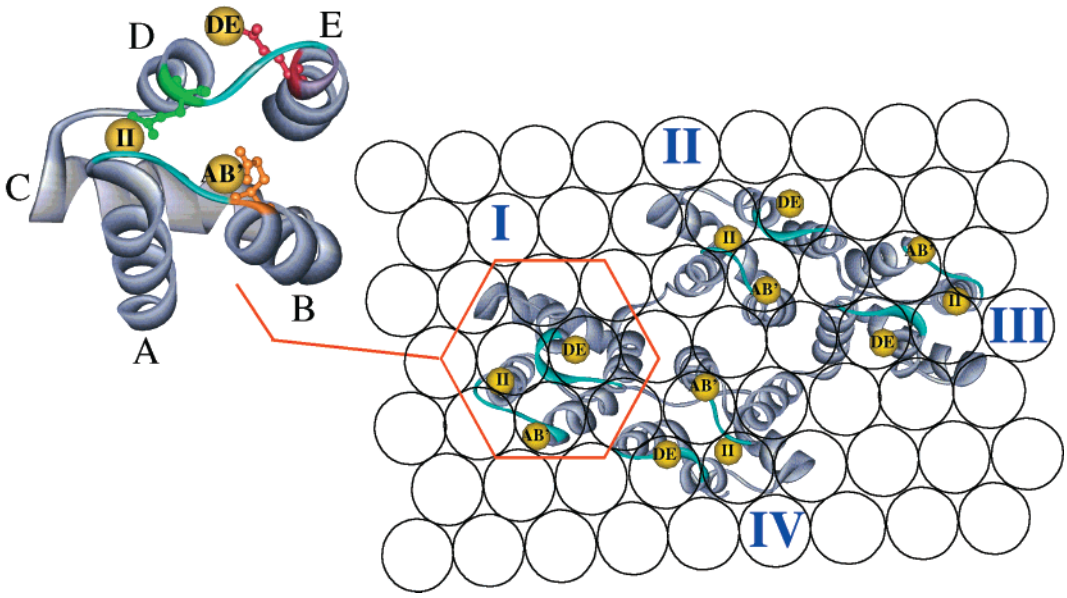

FIGURE 4: Ca^{2+} -dependent membrane binding of ANX. The crystal structure for the soluble form of ANX5 [PDB entry 1A8A (*10*)] with its 10 Ca^{2+} sites (yellow) is shown. In addition, Ca^{2+} (yellow) was modeled into the DE and AB′ sites in repeat 4. The enlarged view of the first repeat shows the carboxylate side chains of the amino acids involved in each of the Ca^{2+} sites: type II in green, DE in red, and AB′ in orange. The circles superimposed over the crystal structure represent phospholipids hexagonally packed at the density (70 Å^2) of a fluid bilayer (*35*). Note the apparent complementarity between the spacing of the Ca^{2+} sites and the spacing of the phospholipids. The face of the soluble protein that contains the Ca^{2+} sites is slightly convex, and it is assumed that small interdomain movements occur upon membrane binding to allow the Ca^{2+} sites to be coplanar (*5*). The exact effect of this putative movement on the spacing of the Ca^{2+} sites is not yet known.

range at which they underwent the transition from the gel to the liquid crystal phase.

In subsequent experiments, ANX12 was incubated with Ca^{2+} and either DMPS/DTPC or DMPG/DTPC vesicles at 37 °C for 15 min. The samples were then cooled to 4 °C, and the level of binding to the vesicles was measured over time. Even after incubation of the samples for 45 min at 4 °C, a temperature that should induce a gel phase transition, there was an only 6% decrease in the total level of ANX12 Ca^{2+}-dependent binding (data not shown).

DISCUSSION

In response to Ca^{2+}, ANX12 changes from a soluble monomer to a peripheral membrane-bound trimer on a millisecond time scale (*18*), suggesting that its physiological role could involve a rapid sensing of intracellular Ca^{2+} concentrations. To evaluate this notion further, we systematically analyzed the Ca^{2+} and phospholipid dependence of ANX12 membrane interaction. We found that ANX12 binds up to 12 Ca^{2+} ions (Figure 2 and Table 1) with remarkable cooperativity (Hill constant $\sim$ 7, Figure 1). Furthermore, the amount of Ca^{2+} required for phospholipid binding of ANX12 is large ($\sim$20 μM) relative to the overall cytosolic Ca^{2+} concentration. However, higher Ca^{2+} concentrations typically occur transiently in the proximity of Ca^{2+} channels (*26*). Thus, ANX12 possesses all of the properties one would expect from a rapid Ca^{2+} sensor, i.e., a rapid and highly cooperative response with the appropriate set point to detect transient spikes of Ca^{2+} near Ca^{2+} channels in the plasma membrane.

ANX12 is known to selectively localize to battery cells in hydra tentacles (*27*). Nematocytes are embedded in the battery cells and contain specialized projectiles used to capture prey in a process that involves an extremely rapid all-or-none Ca^{2+}-dependent exocytic event (*28*). Although the biological function of ANX12 has not been defined, its in vitro properties are well suited to being involved in this process.

What could be the structural basis of ANX12's precisely tuned, rapid, and highly cooperative Ca^{2+} response? On the basis of the location of Ca^{2+} in the X-ray structures of the soluble forms of several ANXs, it is possible to speculate about the location of the Ca^{2+} binding sites in membrane-bound ANX12. Preparation of crystals of most ANX gene products in the presence of high concentrations of Ca^{2+} usually leads to occupancy of at least some classical type II Ca^{2+} sites, and these sites clearly play a critical role in membrane-binding ANXs (*4*−*10*). These high-affinity sites are formed by joint coordination of the cation by backbone carbonyls in the loop between the A and B helices and by a carboxylate side chain in the loop between the D and E helices (*10*). However, two other types of low-affinity Ca^{2+} sites also have been observed in some crystal forms. One type of site is termed AB′ and utilizes carboxylate side chains near the beginning of the B helix, and the other is termed DE and utilizes residues approximately one turn from the beginning of the E helix (see Figure 4 and refs *1* and *10*). It should be emphasized that ANXs have a very low affinity for Ca^{2+} in the absence of phospholipid bilayers. Thus, functional Ca^{2+} binding sites apparently are often unoccupied in the crystal structures. For example, the amino acid sequence of ANX12 reveals the canonical structures for all three types of Ca^{2+} binding sites in each of the four repeats (*16*). Despite the presence of these sites, the crystal structure of ANX12 shows only partial occupancy of the sites with Ca^{2+} in three of the four type II sites plus a Ca^{2+} in one AB′ site and in one DE site (*7*). The ANX crystal structure

that has maximal Ca^{2+} occupancy is that of rat ANX5 [PDB entry 1A8A (*10*)] and contains 10 Ca^{2+}, four type II, three AB′, and three DE sites. This crystal structure is shown in Figure 4 along with two additional Ca^{2+} sites that were modeled into the two remaining sites that were unoccupied. The matrix of circles superimposed over the protein model with the 12 Ca^{2+} sites represents the phospholipids hexagonally packed at the density expected in a fluid phospholipid bilayer. Note that there appears to be a complementarity between the spacing of the Ca^{2+} sites and the spacing of the phospholipids. Each of the 12 Ca^{2+} sites is expected to form a high-affinity bridge that links the protein to the polar headgroup of the lipid. The footprint of the ANX monomer covers approximately 26 phospholipids in a monolayer, so approximately half of the lipid molecules would be anchored to the protein via a Ca^{2+} bridge. Previous studies showed that ANX12 formed trimers on the surface of phospholipid bilayers (*18*). It is interesting to note that the complementarity between the spacing of the ANX12 Ca^{2+} sites and the phospholipid translates across the trimer (not shown), a feature that could contribute to the high stability of the trimer.

Cooperativity in proteins typically requires an initial binding event resulting in a protein conformational change, which in turn alters the affinity for subsequent ligand binding events at other sites. It is possible that such a mechanism could at least in part be operative in ANX12. However, the complementarity between the location of the Ca^{2+} binding sites in ANX12 and the phospholipid structure in bilayers provides an additional explanation for the high Hill constant (Figure 1). It is possible that the formation of a single Ca^{2+} bridge is unfavorable; however, once the bridge is formed, the complementarity between the protein and the phospholipid geometry would significantly facilitate the rapid occupancy of the remaining sites.

The complementarity between phospholipid spacing and the arrangement of the ANX12 Ca^{2+} binding sites noted in Figure 4 has several implications for protein−membrane interaction. If the Ca^{2+} interaction indeed requires the regularly spaced phospholipids, the affinity of ANX12 for Ca^{2+} in the absence of phospholipid should be weak. In fact, this is a well-known feature of ANXs (*1*). Also, ANX12 should only have weak affinity for derivatives of phospholipids that lack the acyl chains. We indeed find this to be the case (J. M. Isas et al., unpublished data). Perhaps most importantly, electrostatic effects would be necessary, but not sufficient, for membrane interactions because, in addition to Coulombic interactions, the charges on the headgroups must be located with spacing that correctly matches that of the ANX12 binding loops. To test this notion, we used PS and PG containing saturated acyl chains to make vesicles that underwent phase transition near room temperature and then evaluated ANX12 binding to these vesicles as a function of temperature. The rationale for this experiment is that at higher temperatures the headgroup spacing of the phospholipid headgroups matches that of ANX12, whereas at lower temperatures, the spacing decreases significantly (*29*). ANX12 bound to these vesicles efficiently only at temperatures above the phase transition (Figure 3). Considering that the Ca^{2+}-dependent membrane interaction of ANXs involves little or no membrane penetration (*18*), we conclude that the temperature-dependent changes in binding affinity were largely due to the altered headgroup arrangement or spacing rather than changes occurring in the acyl chains in the hydrophobic core of the bilayer. We also considered the possibility that ANX12 binding to vesicles composed of PC and acidic phospholipids required the sequestration of the acidic phospholipids under the protein and that binding to vesicles composed of saturated phospholipids did not occur at low temperatures because the lack of lateral mobility prevented sequestration of the acidic phospholipids. However, ANX12 did not bind at low temperatures to vesicles containing only saturated PS and no PC (data not shown), so the lack of binding is not due to inhibition of lateral separation of phospholipids below the phase transition temperature.

The interactions of ANXs with bilayers previously have been studied by several different methods, and it is worthwhile to review these observations in light of the current study of ANX12. A number of these studies observed restricted mobility of bilayer lipid in a manner that can be explained by the extensive interactions between ANX and the bilayer depicted in the model shown in Figure 4. For example, previous fluorescence recovery after photobleaching experiments showed that the phosphatidylserine was nearly laterally immobilized in the presence of ANX5 and Ca^{2+} (*12*), and similar results were obtained with ANX4 interaction with phosphatidylglycerol-containing bilayers (*30*). In addition, our site-directed spin labeling studies of ANX12 indicate strong immobilization of spin-labels placed on loop residues at sites predicted by the model to project toward the bilayer (J. M. Isas et al., unpublished results). Since a fluid bilayer should not cause immobilization of these spin-labels on the EPR time scale, it appears that the formation of the ternary protein−Ca^{2+}−phospholipid complex causes strong immobilization of the phospholipid headgroups. ITC studies showed that Ca^{2+}-dependent binding of ANX12 to phospholipid bilayers was highly exothermic with an enthalpy of association of -75 ± 5 kcal/mol of protein (Figure 2). Since there are ~12 Ca^{2+} sites per monomer (Figure 2 and Table 1), the average enthalpy associated with each Ca^{2+} site is approximately −6 kcal. These data are consistent with a high-affinity binding process with interactions that are strong enough to account for the observed immobilization of bilayer lipids. However, the immobilization does not appear to extend to acyl chains in the core of the bilayer. An EPR spectroscopy study of spin-labels attached to the polar headgroup or at various depths in the acyl chains showed ANX5-dependent membrane rigidity at the surface of the bilayer and at intermediate depths but insignificant effects on fluidity at the core of the bilayer (*31*). An absence of effects of ANX5 binding on the lipid acyl chain flexibility in membranes also was observed in studies using NMR (*32*) and bulk phase infrared spectroscopy (*33*) methods. Taken together, these studies of ANXs on bilayers provide a wealth of information but still do not elucidate the exact nature of the physical change that occurs during the phase transition that prevents ANX12 binding to the gel phase of bilayers.

In summary, it appears that ANX12 has all of the features required for rapid Ca^{2+} sensing and the unique ANX fold appears to be optimized for interaction with phospholipid membranes. Additional studies are needed to determine whether these features are generally applicable to other ANXs.

ACKNOWLEDGMENT

We gratefully thank Dr. James E. Hall and Dr. Kenneth J. Longmuir for insightful discussions.

REFERENCES

1. Seaton, B. A. (1996) in *Annexins: Molecular Structure to Cellular Function* (Seaton, B. A., Ed.) R. G. Landes Co., Austin, TX.
2. Gerke, V., and Moss, S. E. (1997) *Biochim. Biophys. Acta 1357*, 129−154.
3. Liemann, S., and Huber, R. (1997) *Cell. Mol. Life Sci. 53*, 516−521.
4. Weng, X., Luecke, H., Song, I. S., Kang, D. S., Kim, S. H., and Huber, R. (1993) *Protein Sci. 2*, 448−458.
5. Voges, D. B., Burger, R., Demange, A., Baumeister, P., and Huber, R. W. (1994) *J. Mol. Biol. 238*, 199−213.
6. Sopkova, J., Renouard, M., and Lewit-Bentley, A. (1993) *J. Mol. Biol. 234*, 816−825.
7. Luecke, H., Chang, B. T., Mailliard, W. S., Schlaepfer, D. D., and Haigler, H. T. (1995) *Nature 378*, 512−515.
8. Favier-Perron, B., Lewit-Bentley, A., and Russo-Marie, F. (1996) *Biochemistry 35*, 1740−1744.
9. Burger, A., Berendes, R., Liemann, S., Benz, J., Hofmann, A., Gottig, P., Huber, R., Gerke, V., Thiel, C., Romisch, J., and Weber, K. (1996) *J. Mol. Biol. 257*, 839−847.
10. Swairjo, M. A., Concha, N. O., Kaetzel, M. A., Dedman, J. R., and Seaton, B. A. (1995) *Nat. Struct. Biol. 2*, 968−974.
11. Evans, T. C., Jr., and Nelsestuen, G. L. (1994) *Biochemistry 33*, 13231−13238.
12. Cézanne, L., Lopez, A., Loste, F., Parnaud, G., Saurel, O., Demange, P., and Tocanne, J. (1999) *Biochemistry 38*, 2779−2786.
13. Brisson, A., Mosser, G., and Huber, R. (1991) *J. Mol. Biol. 220*, 199−203.
14. Brisson, A., Bergsma-Schutter, W., Oling, F., Lambert, O., and Reviakine, I. (1999) *J. Cryst. Growth 196*, 456−470.
15. Reviakine, I. B.-S., and Brisson, A. (1998) *J. Struct. Biol. 121*, 356−361.
16. Schlaepfer, D. D., Fisher, D. A., Brandt, M. E., Bode, H. R., Jones, J. M., and Haigler, H. T. (1992) *J. Biol. Chem. 267*, 9529−9539.
17. Mailliard, W. S., Leucke, H., and Haigler, H. T. (1997) *Biochemistry 36*, 9045−9050.
18. Langen, R., Isas, J. M., Lueke, H., Haigler, T. H., and Hubbell, W. L. (1998) *J. Biol. Chem. 273*, 22453−22457.
19. Kohler, G., Hering, U., Zschoring, O., and Arnold, K. (1997) *Biochemistry 36*, 8189−8194.
20. Langen, R., Isas, J., Hubbell, W., and Haigler, H. (1998) *Proc. Natl. Acad. Sci. U.S.A. 95*, 14060−14065.
21. Isas, J. M., Cartailler, J. P., Sokolov, Y., Patel, D. R., Langen, R., Luecke, H., Hall, J. E., and Haigler, H. T. (2000) *Biochemistry 39*, 3015−3022.
22. Sokolov, Y., Mailliard, W. S., Tranngo, N., Isas, M., Luecke, H., Haigler, H. T., and Hall, J. E. (2000) *J. Gen. Physiol. 115*, 571−582.
23. Reeves, J. P., and Dowben, R. M. (1969) *J. Cell. Physiol. 73*, 49−60.
24. Tait, J. F., Gibson, D., and Fujikawa, K. (1989) *J. Biol. Chem. 264*, 7944−7949.
25. Blackwood, R. A., and Ernst, J. D. (1990) *Biochem. J. 266*, 195−200.
26. Neher, E. (1995) *Neuropharmacology 34*, 1423−1442.
27. Schlaepfer, D. D., Bode, H. R., and Haigler, H. T. (1992) *J. Cell Biol. 118*, 911−928.
28. Holstein, T., and Tardent, P. (1984) *Science 223*, 830−833.
29. Cevc, G. (1993) *Phospholipids Handbook*, pp 988, Marcel Dekker, Inc., New York.
30. Gilmanshin, R., Creutz, C. E., and Tamm, L. K. (1994) *Biochemistry 33*, 8225−8232.
31. Megli, F. M., Selvaggi, M., Liemann, S., Quagliariello, E., and Huber, R. (1998) *Biochemistry 37*, 10540−10546.
32. Saurel, O., Cézanne, L., Milon, A., Tocanne, J., and Demange, P. (1998) *Biochemistry 37*, 1403−1410.
33. Wu, F., Flach, C. R., Seaton, B. A., Mealy, T. R., and Mendelsohn, R. (1999) *Biochemistry 38*, 792−799.
34. Hill, A. V. (1910) *J. Physiol. 40*, 4−7.
35. Lewis, A. S., and Engelman, D. M. (1983) *J. Mol. Biol. 166*, 211−217.

BI010345+